Artificial Neural Networks based SPWM technique for speed control of Permanent Magnet Synchronous Motor

Suresh Kumar Tummala [1,*] and *Dhasharatha* G [2]

[1]Professor, EEE Department, GRIET, Hyderabad, India
[2] Research Scholar, EEE Department, TKR Engineering College, Hyderabad

Abstract. The advancement of industry apparatuses for some methods with specific tasks to control the working of a few actuators on the field. Among these actuators, Permanent magnet synchronous motor drives are a mainly all-inclusive machine. Proficient utilization of hesitance torque, generally effectiveness, minor misfortunes and smaller size of the motor are the principle attractions of PMSM when contrasted and different drivers. Precise and rapid torque reaction is one of the parameters to determine differentiating arrangements in the ongoing past. The field-situated power perceived the likely and vigorous answer to accomplish these prerequisites to empower the figuring of streams and voltages in different parts of the inverter and motor under transient and consistent conditions. The primary objective of this paper is to investigate Artificial Neural Network based control of speed for PMSM in both open and closed loop under no-load and loaded condition. A shut circle control framework with ANN procedure in the speed circle intended to work in steady torque and transition debilitating districts. MATLAB reproduction performed in the wake of preparing the neural system (directed learning), results for reference control applications are adequate and appropriate in the process business. Speed control in shut circle at different stacking conditions talked about in detail.

1 Introduction

Permanent Magnet Synchronous Motors (PMSM) extensively utilized in low to medium power applications, for example, mechanical autonomy, outer PC flexible speed drives [1], and electric vehicles. The extension in the market of Permanent Magnet (PM) engine drives has requested the requirement for replication instruments fit for taking care of re-enactments for engine drive. Proliferations [2] including engine drives have helped the way toward growing new frameworks by decreasing expense and time. To encourage the improvement of new techniques, recreations of engine drives in a visual situation have the capacities of performing dynamic [3] Simulation.
In this article, a recreation of a field situated controlled [4,5] PM engine drive framework created including every single reasonable segment of the drive framework are introduced. A shut circle control framework with the ANN controller in the speed circle intended to work in consistent torque and motion debilitating locales [6]. Recreation results displayed for two velocities [7] of task, one underneath evaluated and another above-appraised speed.
Artificial Neural Networks are motivated by our present learning of natural sensory systems, in spite of the fact that they don't attempt [8] to be reasonable in everything about (territory of ANN isn't worried about natural demonstrating, an alternate field) [9, 10]. Some ANN models may, along these lines, be unreasonable from an environmental displaying perspective. As opposed to the ordinary advanced PC, ANN plays out their calculation utilizing numerous basic and very interconnected processors working in parallel [11].

2 Mathematical Modelling of PMSM Drive

Vector control likewise read as decoupling or field-orientated control. Vector control decouples three-stage stator current into two-stage d-q hub present, one delivering motion and other creating torque and permits coordinate control of motion and torque. In this way, by utilizing vector control, the PMSM is comparable to an independently energized dc machine. The model of PMSM is nonlinear. Along these lines, by utilizing vector control, the model of PMSM is direct.

For building a pivoting attractive field and drive the rotor, tweaked current provided to the ABC stator windings. The vector control system figured in the synchronously pivoting reference outline, ABC stator arranges, stationary α-β hub organizes and turning d-q hub facilitates equal relations of streams worked by Clarke – Park [4] and backwards changes Fig.1 demonstrates a vector chart of the PMSM. i_d slacks i_q by

* Corresponding author: sureshkumar.t@griet.ac.in

90º; in this way, id must be along the rotor motion. In the event that id is along rotor motion, the d-hub stator transition adds to the rotor motion influencing an expansion of net air hole motion [10].

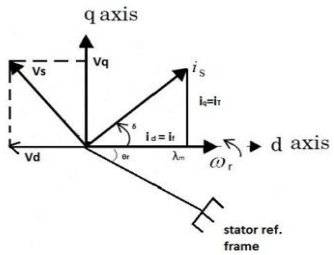

Fig. 1. Phasor representation of PMSM

$$i_a = i_s \sin(\omega_r t + \delta) \quad (1)$$

$$i_b = i_s \sin(\omega_r t + \delta - \frac{2\pi}{3}) \quad (2)$$

$$i_c = i_s \sin(\omega_r t + \delta + \frac{2\pi}{3}) \quad (3)$$

Where $\theta_r = \omega_r t$, from phasor representation we have:

$$\begin{matrix} i_q \\ i_d \end{matrix} = i_s \begin{bmatrix} \sin\delta \\ \cos\delta \end{bmatrix} \quad (4)$$

If $i_d = 0$ by $\delta = 90^\circ$ then the electric torque equation:

$$T_e = \left(\frac{3}{2}\left(\frac{P}{2}\lambda_m i_q\right)\right) \quad (5)$$

A constant torque is attainable if i_q is constant. Hence the electric torque is subject to only on the quadrature axis current.

d axis stator voltage:

$$V_d = Ri + L_d \frac{di_d}{dt} - L_q \omega_e i_q \quad (6)$$

q axis stator voltage:

$$V_q = Ri_q + L_q \frac{di_q}{dt} + L_d \omega_e i_d - \omega_e \lambda_{af} \quad (7)$$

d axis magnetic flux linkage:

$$\lambda_d = L_d i_d + \lambda_{af} \quad (8)$$

q axis magnetic flux linkage:

$$\lambda_q = L_q i_q \quad (9)$$

Electromagnetic torque

$$T_e = J\frac{d}{dt}\omega_r + B\omega_r + T_l \quad (10)$$

From torque equation

$$T_e = \frac{3}{2}P\left(\lambda_{af} i_q + (L_d - L_q) i_d i_q\right) \quad (11)$$

Where $\omega_r = \frac{2}{p}\omega_e$ (12)

Rotor speed in angular frequency

$$\omega_e = \int \frac{1}{\omega_r}\left[\frac{1}{J}\frac{P}{2}(T_e - T_m - B\frac{2}{p}\omega_e)\right] \quad (13)$$

3 Block Diagram Representation

In the event that the quick size of the regulation flag is higher than the bearer motion at a point in time, the yield voltage of the inverter leg should associate with the positive side of the DC connect [6]. In the event that the bearer flag is higher than the adjustment flag, the yield should identify with the negative of the DC interface.

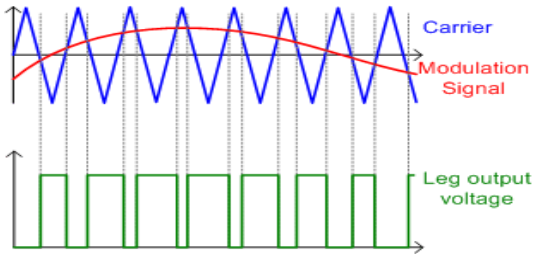

Fig. 2. PWM Principle

From the above approach, the output waveform can be made to follow any desired waveform shape. With machines, sinusoidal and trapezoidal waveform shapes are among the most common. The underlying block diagram representation of PMSM with ANN shown in figure 3. ANN has taken in controller block.

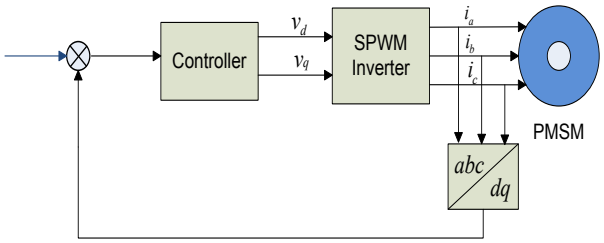

Fig. 3. Block diagram representation of PMSM

4 PMSM with ANN

Multilayer Neural Networks look like the Single Layer Neural Networks besides that despite the data and yield layer, it has no less than one disguised layer. Backpropagation Neural Network is a Multilayer Feed Forward Neural Network which utilizes the broadened inclination plummet-based delta learning standard and known as back proliferation (of mistakes) administer for preparing. The design of a Backpropagation Neural Network appeared in Fig 4.

The system has one info layer, one yield layer, and concealed layers. The information layer is associated with the thick coat and further associated with the yield layer using interconnection weights. In the figure, just a feed forward period of a system appeared, however the blunders backpropagated amid the Backpropagation (of oversights) period of learning, there might be any number of shrouded layers in a framework yet increment in the quantity of concealed layers results in the computational many-sided quality of the net. Subsequently, the time taken for intermingling and to limit the blunder might be high and an inclination accommodated both covered up and yield layer. Parameters pertaining to ANN listed in Table 1 for quick reference.

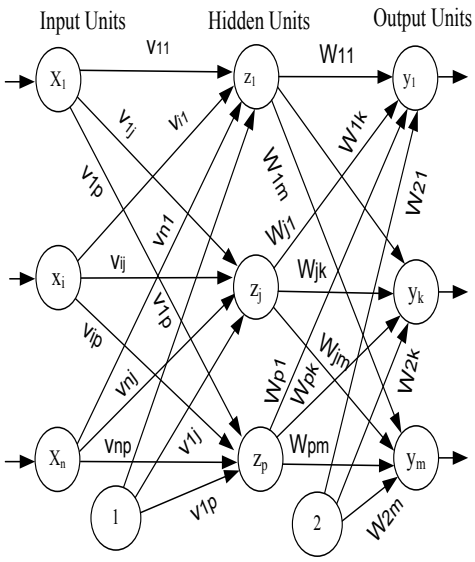

Fig. 4. Backpropagation of Neural Network

The preparation of Backpropagation Neural Network includes four phases including (an) Initialization of weights (b) Feed Forward Phase (c) Backpropagation of blunders (d) Updation of weights and predisposition. Amid the main stage, every one of the weights instated to little arbitrary qualities. In the feed forward stage, each information unit gets an information flag and communicates this message to every one of the concealed gatherings. Every obscure unit at that point processes its initiation and sends its message to each yield unit. Each yield unit figures its initiation to shape the reaction of the net for the given information design. Simulation model and experimental setup of PMSM with ANN presented in Figure 5 and 6.

Table 1. ANN Parameters

Parameter Name	Parameter Value
Hidden layer transfer function	Tansig
Output layer transfer	Purlin
Activation function	Net sum
Gradient	1.2145e-10
No. of weights	10
Regression	1
Training sets	150
Testing sets	110

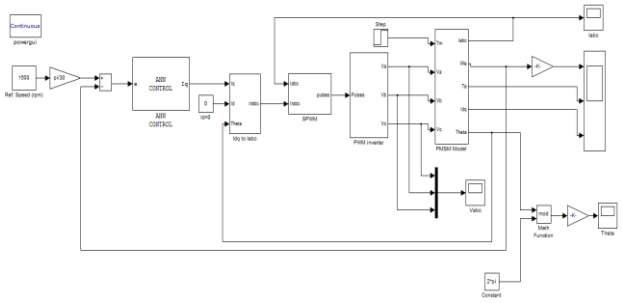

Fig. 5. Simulation model of PMSM with ANN

Fig. 6. Experimental Test bed of PMSM with ANN controller

5 Results and Discussion

In this segment, the reaction of different rates of PMSM under no-load and load of 1N-m connected at 0.05 sec are discussed alongside the reaction of currents of three-phases and two-phase (d, q).

5.1 Speed of 700 rpm under no-load condition

Speed representation of the ANN controller shown in Fig 7. In which speed reaches a maximum and then maintains a constant by taking 700 rpm under a no-load condition.

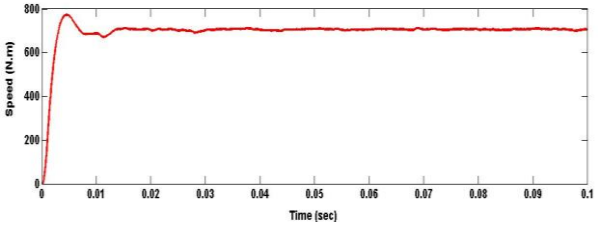

Fig. 7. Speed at 700 rpm under no-load condition

Torque representation of ANN controller shown in Fig 8. In which torque reaches to maximum torque then settled precise instant when the speed at 700 rpm under a no-load condition.

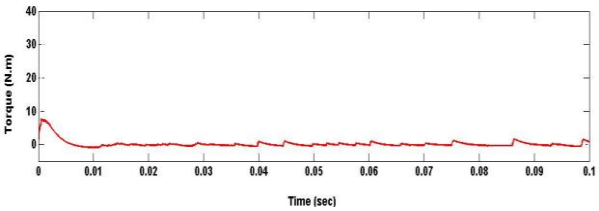

Fig. 8. Torque at 700 rpm under no-load condition

5.2 Speed at 1300 rpm under no-load condition

Speed representation of the ANN controller shown in Fig 9. In which speed reaches a maximum then maintains a constant by taking 1300 rpm under a no-load condition.

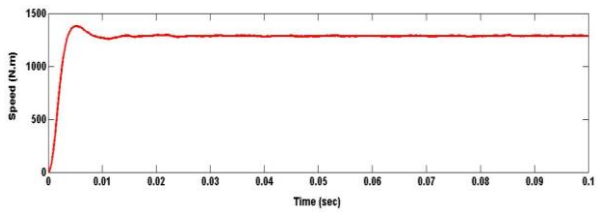

Fig. 9. Speed at 1300 rpm under no-load condition

Torque representation of ANN controller shown in Fig 10. In which torque reaches to maximum torque then settled precise instant when the speed at 1300 rpm under a no-load condition.

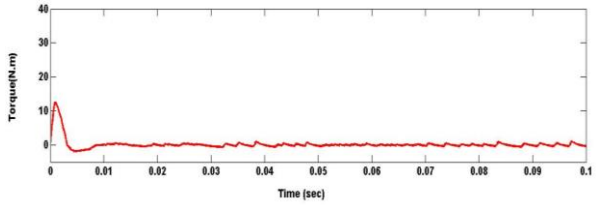

Figure 10. Torque at 1300 rpm under no-load condition

5.3 Speed at 2000 rpm under no-load condition

Speed representation of the ANN controller shown in Fig 11. In which speed reaches a maximum then maintains a constant by taking 2000 rpm under a no-load condition.

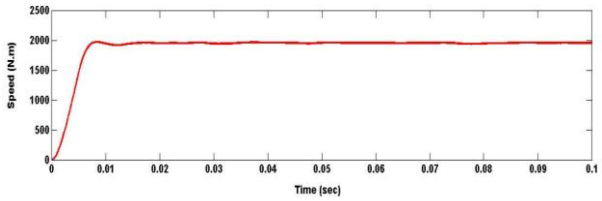

Fig. 11. Speed at 2000 rpm under no-load condition

Torque representation of the ANN controller shown in Fig 12. In which torque reaches to maximum torque then settled precise instant when the speed at 2000 rpm under a no-load condition.

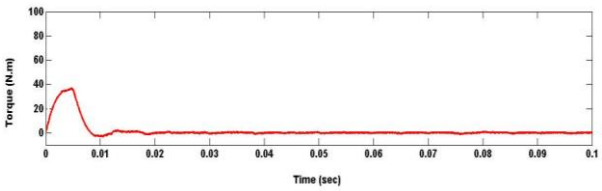

Fig. 12. Torque at 2000 rpm under no-load condition

5.4 Speed at 700 rpm under load condition

Speed representation of the ANN controller shown in Fig 13. In which speed reaches a maximum then maintains a constant by taking 700 rpm under 1 N.m load torque at 0.05 sec.

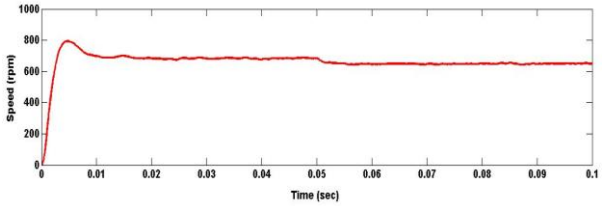

Fig. 13. Speed at 700 rpm under 1 N-m load at 0.05sec

Torque representation of the ANN controller shown in Fig 14. In which torque reaches to maximum torque then settled specific instant when speed at 700 rpm under 1 N.m load torque at 0.05 sec.

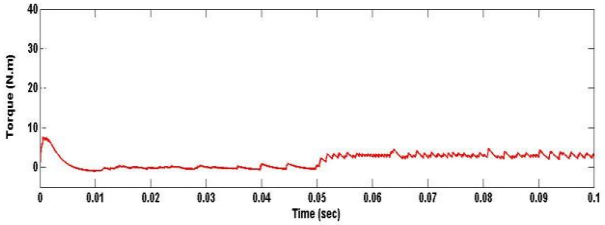

Fig. 14. Torque at 700 rpm under 1 N-m load at 0.05sec

Phase currents (Three & Two) chart is demonstrated as follows in Figure 15 & 16. In PI controller three stage streams have swells yet utilizing of ANN controller there are no swells. d-axis current is nearly equal to zero. q-axis current is away from d-axis as shown in figure 16. So, this strategy is a productive apparatus for controlling reason.

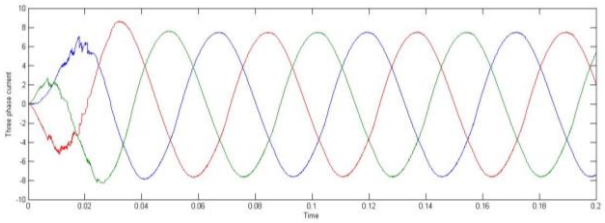

Fig. 15. Three Phase Currents of PMSM with ANN

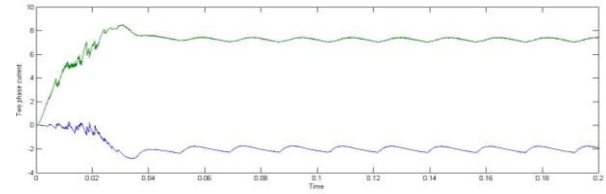

Fig. 16. Two Phase Currents (d, q) of PMSM with ANN

APPENDIX

Table 2. PMSM Specifications

Parameter Name	Parameter Value
Stator Resistance (R)	2.875 Ohm
d-axis self-inductance (L_d)	0.0066 H
q-axis self-inductance (L_q)	0.0058 H
Rotor magnetic flux linkage to the stator (Y_{af})	0.1546 Wb/m^2
Moment of Inertia (J)	0.0176 Kg-m^2
Friction coefficient (B)	0.00038818 N-m/(rad/s)
Number of poles (p)	6
Constant frequency (f)	50Hz
DC link voltage (V_{dc})	150 V
Synchronous speed (N_s)	1000 rpm

6. CONCLUSIONS

This paper talked about numerical demonstrating of executed PMSM drive framework. The concise diagram

of the crucial guideline of sinusoidal heartbeat width balance changing the width of the beats in a heartbeat prepare introduced in this article. The higher the control voltage, the more extensive the subsequent vibrations move toward becoming. Steady adequacy beats describe PWM procedures which are very famous in mechanical applications. The width of these heartbeats is balanced to get inverter yield voltage control and to decrease its symphonious substance.

To enhance the framework power and the capacity of brisk recuperation of the speed from any unsettling influence and parameter variety ANN control system created. ANN-based speed controller model of PMSM drive displayed and reproduced and the outcomes spoke to for Artificial Intelligence-based control. These are intended to make an interpretation of the speed mistakes into separate driving voltage signs to the contribution of PMSM. A multilayer feed forward neural system is prepared utilizing Backpropagation learning calculation to evaluate the driving voltage contribution of PMSM. The reproduced aftereffects of shut circle speed control of ANN speed controller with PMSM have created above and underneath appraised speed at no-heap and full load conditions.

References

1. M. Arehpanahi, M. Fazil, “Position Control Improvement of Permanent Magnet Motor using Model Predictive control”, ***IJE Transactions A: Basics***, Vol. 31, No. 7 (2018), 1044-1049.
2. Zheng Wang, Jian Chen, Ming-Cheng and K. T. Chau, "Field-oriented control & direct torque control for paralleled VSI fed PMSM drives with variable switching frequencies," ***IEEE Transactions on Power Electronics***, Vol. 31, No. 3 (2016), 2417-2428.
3. R. Pilla, A. S. Tummala and M. R. Chintala, “Tuning of Extended Kalman Filter using Self-Adaptive differential evolution algorithm for sensorless permanent magnet synchronous motor drive”, ***IJE Transactions B: Applications***, Vol. 29, No. 11(2016), 1565-1573
4. M. Hinkkanen, T. Tuovinen, L. Hornefors and J. Luomi, "A combination position and stator-resistance observer for salient PMSM drives: Design and stability analysis," ***IEEE Transactions on Power Electronics***, Vol. 27, No. 2 (2013), 601-609.
5. S. Kouro, J. Rodriguez, B. Wu, S. Bernet and M. Perez, "Powering the future of the industry: high power adjustable speed drive topologies," ***IEEE Industry Magazine***, 2012, 26-39.
6. Z. Pan and R. A. Bharat, "Modular motor/converter system with redundancy for high speed, high power motor applications***," IEEE Transactions on Power Electronics***, vol. 25, no. 2 (2010), 408-416.
7. Junjie, Ren, HuiFeng, HongyingRen and Yi Huang, “Simulation of PMSM vector control system based on propeller load characteristic," Proceeding of the IEEE International conference on intelligent control and information processing, Aug 13-15, 2010, pp. 735-737.
8. R. Krishnan, Permanent magnet synchronous and brushless DC motor drives, USA: Boca Raton, (2010).
9. X. Xiao, C. M. Chen, and M. Zhang, "Dynamic permanent magnet flux estimation of permanent magnet synchronous machines," ***IEEE Transactions on Applied Superconductor***. Vol. 2, No. 3 (2010), 1085-1088.
10. J. Soltani, NR Abjadi, M. Pahlavaninezhad, "An adaptive nonlinear controller for speed sensorless PMSM taking the iron loss resistance into account," ***IJE Transactions B: Applications***, vol. 21, no. 2 (2008), 151-160.
11. M. Rashed, P. F. A. Macconnell, A. F.Stronach and P. Acarnely, "Sensorless indirect rotor field orientation speed control of permanent magnet synchronous motor with stator resistance estimation," ***IEEE Transactions on Industrial Electronics***, vol. 54, no. 3 (2007), 1664-1675.